Determinants of Excitability in Cardiac Myocytes: Mechanistic Investigation of Memory Effect

Thomas J. Hund* and Yoram Rudy*†‡

Cardiac Bioelectricity Research and Training Center and Departments of Biomedical Engineering,* Physiology & Biophysics,† and Medicine,‡ Case Western Reserve University, Cleveland, Ohio 44106-7207 USA

ABSTRACT The excitability of a cardiac cell depends upon many factors, including the rate and duration of pacing. Furthermore, cell excitability and its variability underlie many electrophysiological phenomena in the heart. In this study, we used a detailed mathematical model of the ventricular myocyte to investigate the determinants of excitability and gain insight into the mechanism by which excitability depends on the rate and duration of pacing (the memory effect). Results: i) The primary determinant of excitability depends upon the duration (T) of the stimulus. ii) For a short T, excitability is determined by the difference between the threshold membrane potential and the resting membrane potential. iii) For a long T, excitability is determined by the resting membrane resistance, R_m. iv) In the case of long T, pacing induced changes in $[Na^+]_i$ and $[Ca^{2+}]_i$ over time affect R_m and excitability by shifting the current-voltage (IV) curve in the vertical direction and are responsible for the memory effect. Conclusions: The results have important implications during an arrhythmia, where a cardiac cell may be subjected to rapid repetitive excitation for an extended period of time. Effective anti-arrhythmic strategies may be developed to exploit the R_m dependence of excitability for a long T.

INTRODUCTION

Cell excitability has been defined as "the ease with which a response may be triggered" (Boyett and Jewell, 1980). It is known that the excitability of a cardiac cell is variable and depends on the coupling interval, or timing of stimulation relative to a previous action potential (AP). This dependence may be characterized by the strength-interval (SI) curve (Spear and Moore, 1974; Boyett and Jewell, 1980; Davidenko et al., 1990), which depicts the minimum current stimulus needed to elicit an AP as a function of the coupling interval. Importantly, the SI curve may shift or change morphology in response to changes in extracellular potassium concentration, $[K^+]_o$, and depends on the duration and rate of pacing previous to its measurement (memory effect). In fact, a paradoxical increase in excitability (supernormal excitability) has been reported experimentally during rapid pacing, when the transmembrane potential (V_m) at rest ($V_{m,rest}$) is slightly depolarized (Davidenko et al., 1990). Supernormal excitability has also been observed during mild hyperkalemia, where a moderate elevation of $[K^+]_o$ leads to a depolarization of $V_{m,rest}$ and an increase in conduction velocity (Dominguez and Fozzard, 1970; Buchanan et al., 1985; Shaw and Rudy, 1997a). (See Table 1 for an explanation of abbreviations used in this paper.)

We define "memory" as the dependence of a cell's behavior on its past history. This general definition of memory encompasses various specific forms of memory such as T-wave change following a period of ventricular pacing (cardiac memory; Rosenbaum et al., 1982) or the memory effect discussed in this study, where the pacing history of a cell alters its excitability.

Excitability and its variability underlie many electrophysiological phenomena in the heart. For example, the presence of supernormal excitability can cause the appearance of arrhythmogenic, chaotic dynamics in rapidly paced cardiac cells (Chialvo et al., 1990; Luo and Rudy, 1991). At a more fundamental level, the conduction velocity of an AP propagating through cardiac tissue increases with increasing excitability (Spear and Moore, 1974; Peon et al., 1978). This dependence of cellular responses and of AP conduction on excitability implies its critical role in cardiac excitation and arrhythmias. However, despite this fundamental significance, the biophysical determinants of excitability are not clearly understood. In fact, there is still a conflict in the literature as to the determinants of supernormal excitability. Davidenko et al. (1990) suggest that the resting membrane resistance, R_m, is the primary determinant of supernormal excitability observed in rapidly paced guinea pig papillary muscle. According to this hypothesis, rapid pacing depolarizes $V_{m,rest}$, which leads to an increase in R_m due to the rectification property of I_{K1}. In this scheme, the relationship between R_m and I_{th} becomes clear if we define I_{th} as the current required to establish a V_m equal to the threshold voltage, V_{th}, at which an AP will be generated. For a larger R_m, a smaller I_{th} current is needed to reach a given V_{th}. Other studies propose that supernormality is due to a decrease in the difference, ΔV, between $V_{m,rest}$ and V_{th} (Dominguez and Fozzard, 1970; Spear and Moore, 1974; Buchanan et al., 1985; Shaw and Rudy, 1997a). In this scenario, a moderate depolarization of $V_{m,rest}$ decreases ΔV, thereby reducing the stimulus charge needed to elevate V_m to V_{th} by charging the membrane capacitance.

Received for publication 18 April 2000 and in final form 6 September 2000.

Address reprint requests to Yoram Rudy, Director, Cardiac Bioelectricity Research and Training Center, 319 Wickenden Building, Case Western Reserve University, Cleveland, OH 44106-7207. Tel: 216-368-4051; Fax: 216-368-4969; E-mail: yxr@po.cwru.edu.

0006-3495/00/12/3095/10 $2.00

TABLE 1 Abbreviations and definitions

AP	Action potential
DI	Diastolic interval
SI curve	Strength-interval curve
R_m	Resting membrane resistance
C	Membrane capacitance
V_m	Membrane potential
I	Transmembrane current
I_{th}	Threshold current for excitation
T	S2 stimulus duration
V_{th}	Threshold transmembrane potential
ΔV	$V_{th} - V_{m,rest}$
I_{stim}	Stimulus current
I_{NaK}	Sodium-potassium pump
I_{NaCa}	Sodium-calcium exchanger
I_{Na}	Fast sodium current
I_{K1}	Inward rectifying potassium current
$\bar{g}_{Na}$	Maximum conductance of I_{Na}
$\bar{g}_{K1}$	Maximum conductance of I_{K1}
E_{K1}	Reversal potential of I_{K1}
τ_h	Time constant of fast I_{Na} inactivation
S1	Pacing stimulus
S2	Test stimulus
S1S1	Pacing interval (basic cycle length)
S1S2	Coupling interval

The objectives of this investigation are to understand the fundamental determinants of excitability and to gain insight into the mechanism by which excitability depends on the duration and rate of pacing (the "memory effect") using a comprehensive model of the cardiac ventricular cell. Since excitability is instrumental in determining the behavior of the cell both in isolation and in the multicellular tissue, understanding its mechanism and its dependence on pacing history (memory effect) may provide fundamental insights into processes that govern AP generation and propagation in the heart. Furthermore, accumulation of intracellular Na^+ and Ca^{2+} during rapid pacing is known to be arrhythmogenic (Ravens and Himmel, 1999; Faber and Rudy, 2000). Therefore, a model that accurately describes changes in intracellular ion concentrations and their effects on excitability may provide a mechanistic insight into arrhythmogenesis.

METHODS

The cardiac ventricular cell model

The Luo-Rudy theoretical model (Luo and Rudy, 1994a; Zeng et al., 1995; Viswanathan et al., 1999; Faber and Rudy, 2000) is used to simulate the single-cell AP (Fig. 1 *A*). The model accounts for dynamic intracellular concentration changes of Na^+, K^+, and Ca^{2+} and includes ion pumps and exchangers responsible for maintaining cell homeostasis (important to this study are the sodium-potassium pump, I_{NaK}, and the sodium-calcium exchanger, I_{NaCa}). To examine the memory effect, an S1S2 pacing protocol is used (schematically depicted in Fig. 1 *B*). In this protocol, the cell is paced at a set rate (S1S1 interval) by an S1 stimulus of constant amplitude and duration. Following the last S1 stimulus, an S2 stimulus of varying amplitude and duration (T) is applied to the cell at a variable S1S2 coupling interval. The S1S1 interval is varied (either 150 ms or 300 ms) to examine the rate dependence of excitability, and the number of applied S1 stimuli is varied (either 100 or 2000 beats) to examine the dependence of excitability on the duration of pacing. Table 2 summarizes the data from the pacing protocols.

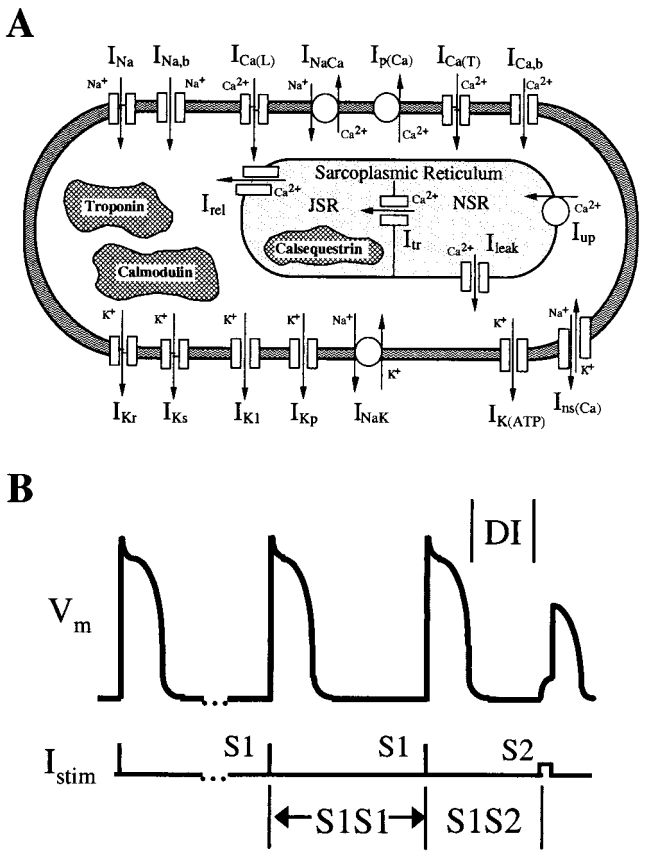

FIGURE 1 (*A*) Schematic of the Luo-Rudy cell model depicting the various ion channels, pumps, and exchangers represented in the model. Details of the model and definition of its parameters are provided in the literature (Luo and Rudy, 1994a; Zeng et al., 1995; Shaw and Rudy, 1997b; Viswanathan et al., 1999; Faber and Rudy, 2000). Selected parameters are defined in Table 1. (*B*) Schematic showing S1S2 pacing protocol. The cell is paced at an S1S1 interval for a period of time, after which an S2 stimulus is applied at different coupling intervals.

The strength-interval (SI) curve

SI curves are created by calculating I_{th} for a wide range of S1S2 coupling intervals. For simplicity during detailed investigation of the memory effect, an S2 is applied after a diastolic interval (DI) of 430 ms (a DI of intermediate duration). The phenomenon of interest (the memory effect)

TABLE 2 Intracellular ion concentrations after different pacing protocols

Pacing protocol (S1S1/# of beats)	$[Na^+]_i$ (mM)	$[Ca^{2+}]_i$ (μM)	$[K^+]_i$ (mM)
150 ms/100 beats	10.550	0.290	142.89
300 ms/100 beats	10.995	0.148	143.19
150 ms/2000 beats	14.124	0.340	132.51

occurs over a wide range of DIs and the particular choice does not affect the conclusions of this study.

Stimulus characteristics

The S1 stimulus is a current pulse with a duration of 0.5 ms and magnitude approximately twice diastolic threshold (a diastolic threshold $\cong$ 70 μA/μF is the smallest stimulus required to elicit an AP in the resting cell). The membrane resistance, R_m, is calculated with an S2 voltage clamp to 10 mV above $V_{m,rest}$ for 50 ms, after which V_m is allowed to return to rest. The time required for V_m to decay to 1/e its peak value is the time constant of the membrane ($\tau = R_mC$) from which R_m is calculated; the membrane capacitance, C, is 1 μF/cm^2 (Weidmann, 1952; Dominguez and Fozzard, 1970; Jack et al., 1983).

Excitability is determined by finding the minimum S2 stimulus current (I_{th}) required to initiate an AP with T = 1, 5, 20, or 40 ms. A wide range of T is used to investigate the relationship between T and the determinants of excitability. An S2 pulse with T = 20 ms duration is used to create the SI curve, following experimental procedures (Davidenko et al., 1990).

ΔV is defined as ($V_{th} - V_{m,rest}$), where V_{th} is the minimum voltage amplitude of a 0.5 ms voltage clamp pulse which generates an AP. $V_{m,rest}$ is the diastolic potential just before the S2 stimulus is applied.

Current-voltage curve

The membrane current-voltage (IV) curve is created by stepping the membrane to a given voltage for 2 ms, after which the total membrane current is recorded. In addition to the voltage step protocol mentioned previously, R_m is calculated from the IV curve as the inverse of the slope about V_0 ($V_m = V_0$ where I = 0) over a 2 mV range. For long T, I_{th} is also determined from the IV curve as the current passing through the membrane resistance when $V_m = V_{th}$.

Cell model modifications

In certain simulations, to gain insight into the determinants of excitability we independently altered R_m and ΔV as follows. The fast sodium current, I_{Na}, determines the rapid AP upstroke but not the rest potential. Therefore, altering its conductance, $\bar{g}_{Na}$, alters V_{th} without affecting R_m at rest. The inwardly rectifying potassium current, I_{K1}, is primarily responsible for maintaining $V_{m,rest}$ and changing its conductance, $\bar{g}_{K1}$, affects R_m without significantly affecting V_{th}. Furthermore, we change $\bar{g}_{K1}$ immediately before application of the stimulus so that $V_{m,rest}$ (and therefore ΔV) does not change significantly.

We also use ion reset protocols in which $[Na^+]_i$ and $[Ca^{2+}]_i$ are reset to previous values during pacing. During the $[Ca^{2+}]_i$ reset protocol, intracellular stores of Ca^{2+} and buffered Ca^{2+} are reset as well.

RESULTS

Dependence of excitability on pacing history: strength-interval curves

The dependence of excitability on the cell's pacing history (the memory effect) is illustrated in Fig. 2. After pacing at a basic cycle length of 150 ms (rapid pacing), the SI curve is shifted downward and to the left relative to the curve measured after pacing the cell at a basic cycle length of 300 ms (normal pacing rate, typical of guinea pig heart rate at rest), a phenomenon that is consistent with experiment (Davidenko et al., 1990). The leftward shift of the SI curve

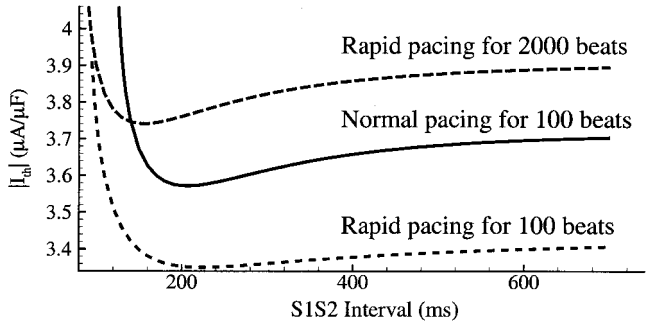

FIGURE 2 The dependence of the strength-interval (SI) curve on the rate and duration of pacing. The SI curve shows I_{th} as a function of the S1S2 coupling interval. SI curves are generated after pacing the cell 100 times at an S1S1 of 150 ms (*short dashed line*) and of 300 ms (*solid line*), and after pacing 2000 times at an S1S1 of 150 ms (*long dashed line*).

reflects shortening of action potential duration at the fast rate, a phenomenon known as rate adaptation, which allows for elicitation of an AP at smaller coupling intervals. The downward shift indicates an increase in excitability as observed experimentally (Davidenko et al., 1990). After a longer period (2000 beats) of rapid pacing, the SI curve shifts to the left and upward relative to that after the 100th stimulus at the same rate. The upward shift of the SI curve indicates a decrease in excitability as the cell is paced for longer periods of time.

Relative importance of R_m and ΔV in determining excitability: a linear circuit analysis

We gain insight into the determinants of excitability and the mechanism responsible for the memory effect (Fig. 2) by assuming that i) the membrane at rest is a linear RC circuit (schematic in Fig. 3), and ii) during a step-function stimulus, V_{th} increases exponentially (accommodation; Noble and Stein, 1966; Jack et al., 1983) with a time constant τ_h, due to inactivation of I_{Na}. For the sake of simplicity, the reversal potential (E_{K1}) of I_{K1} is set to zero. Inclusion of E_{K1}

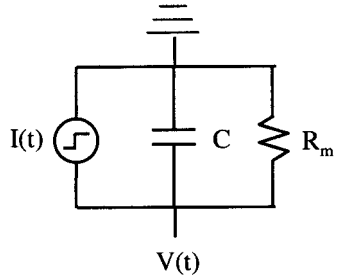

FIGURE 3 Equivalent circuit representing the resting membrane. I(t) is the current step applied to stimulate an AP and can be represented mathematically as $I_{stim} \cdot U(t)$ where U(t) is a step function. The circuit represents the membrane resistance (R_m) in parallel with the membrane capacitance (C).

in the following analysis adds only a DC shift to the equations. The general solution to the differential equation governing the response of an RC circuit to a current step with amplitude I_{stim} is given by Eq. 1, where R_mC is the time constant of the circuit and $V_{m,rest}$ is the value of $V_m(t)$ at time $t = 0$.

$$V_m(t) = (V_{m,rest} - I_{stim} \cdot R_m)e^{-t/R_mC} + I_{stim} \cdot R_m \quad (1)$$

According to Assumption 2, the time dependence of V_{th} in response to a current step may be described by Eq. 2, where τ_h is the time constant of inactivation of I_{Na}.

$$V_{th}(t) = V_{th}(0)e^{t/\tau_h} \quad (2)$$

For a particular pulse duration, T, an AP will be generated with a minimum $I_{stim} = I_{th}$ if V_m at time $t = T$ is equal to V_{th} of Eq. 2. Setting Eq. 1 equal to Eq. 2, substituting I_{th} for I_{stim}, and solving for I_{th} results in Eq. 3,

$$I_{th} = (V_{th}(0)e^{T/\tau_h} - V_{m,rest}e^{-T/R_mC})/(R_m(1 - e^{-T/R_mC})) \quad (3)$$

We assume that V_m reaches steady state before I_{Na} shows appreciable inactivation ($\tau_h \gg R_mC$) and examine the implications for I_{th} over a range of pulse duration, T.

Theoretical analyses of cable excitation have assumed short T (Noble and Stein, 1966; Jack et al., 1983). In this study, we examine excitability over a wide range of T. Under circumstances where $\tau_h \gg R_mC$, we consider three ranges of T: a very short stimulus, ($T \ll R_mC \ll \tau_h$); a stimulus of intermediate duration, ($R_mC \ll T \ll \tau_h$); and a very long stimulus, ($R_mC \ll \tau_h \ll T$).

For a current stimulus with a very short T (Case 1: $T \ll R_mC \ll \tau_h$), the expression $(1 - e^{-T/R_mC})$ in Eq. 3 may be approximated as T/R_mC, and Eq. 3 reduces to Eq. 4,

$$I_{th} = C \cdot \Delta V/T \quad (4)$$

where $\Delta V = V_{th} - V_{rest}$. In this case, ΔV appears explicitly in the formulation for I_{th}, whereas R_m does not. This is because during a short T, the entire stimulus current is used to charge the membrane capacitance. Over this range of T, the magnitude of ΔV determines the amount of charge a stimulus must provide to the membrane to raise V_m to V_{th}.

Next we consider Case 2, where $R_mC \ll T \ll \tau_h$, such that V_m reaches steady state before the end of the stimulus and before V_{th} begins to rise due to inactivation of I_{Na}. In this scenario, Eq. 3 reduces to Eq. 5,

$$I_{th} = V_{th}/R_m \quad (5)$$

I_{th} depends only on R_m and V_{th} and shows no dependence on ΔV. In fact, assuming that R_m changes while V_{th} remains constant, then $I_{th} \propto 1/R_m$ and excitability is determined solely by R_m. In the steady state, the stimulus current passes entirely through the membrane resistance. The voltage at steady state depends on the magnitude of the stimulus current and the membrane resistance but not on the initial value of the membrane voltage, $V_{m,rest}$. Thus, for T longer than the membrane time constant (R_mC), AP generation (excitability) is determined by R_m, not by ΔV.

The relation expressed in Eq. 5 holds also for T much longer than τ_h, assuming that V_m still reaches steady state before appreciable I_{Na} inactivation (Case 3: $R_mC \ll \tau_h \ll T$). In this case, the AP is elicited well before the end of the stimulus and before V_{th} begins to elevate due to appreciable inactivation of I_{Na}.

The linear RC circuit analysis predicts that the primary determinant of excitability depends on T. As T increases, a transition occurs from ΔV-dependent excitability to R_m-dependent excitability. Therefore, we hypothesize that the mechanism responsible for the memory effect of excitability also depends on T.

Relative importance of R_m and ΔV in determining excitability: cell-model simulations

We next test our hypothesis that the primary determinant of excitability depends on T using a realistic, nonlinear model of the cardiac action potential. In Fig. 4, we plot I_{th} (the S2 threshold current for eliciting an AP in the Luo-Rudy model) as a function of R_m and as a function of ΔV for four different values of T (Fig. 4, *A-D*). As T increases, I_{th} undergoes a transition from being more closely correlated with ΔV (Fig. 4 *A*) to being more closely correlated with R_m (Fig. 4, *C* and *D*). The transition from ΔV-dependent to R_m-dependent excitability occurs approximately at T = 5 ms (Fig. 4 *B*). These results are consistent with the hypothesis that as T increases, a transition occurs from ΔV-dependent to R_m-dependent excitability.

To further examine the relative importance of R_m and ΔV in determining excitability, we investigate the effects of independently altering R_m and ΔV on I_{th} for long T (Fig. 5 *A*) and short T (Fig. 5 *B*). In Fig. 5, $\bar{g}_{K1}$ or $\bar{g}_{Na}$ are manipulated (protocol described in Methods) to change R_m or ΔV independently during determination of I_{th} with a S2 stimulus of 1 ms (Fig. 5 *A*) or 20 ms (Fig. 5 *B*).

Eliminating rate-dependent differences in ΔV (by decreasing $\bar{g}_{Na}$ from 16 mS to 10 mS after rapid pacing) reduces the rate-dependent differences in excitability for short T (Fig. 5 *A*, equal ΔV) but has a relatively weak effect for long T (Fig. 5 *B*, equal ΔV). Oppositely, eliminating rate-dependent differences in R_m (by increasing $\bar{g}_{K1}$ from 0.75 mS to 0.80 mS after rapid pacing) is more effective in reducing rate-dependent differences in excitability for long T (Fig. 5 *B*, equal R_m) than for short T (Fig. 5 *A*, equal R_m). It is clear from these results that the determinants of excitability depend on T. Furthermore, these results support the hypothesis that the mechanism of the memory effect is dependent on T.

We have shown above that ΔV is the major determinant of excitability for very short T. In this range of T, a moderate elevation of $V_{m,rest}$ decreases ΔV and, therefore, increases excitability. Further elevation of $V_{m,rest}$ leads to

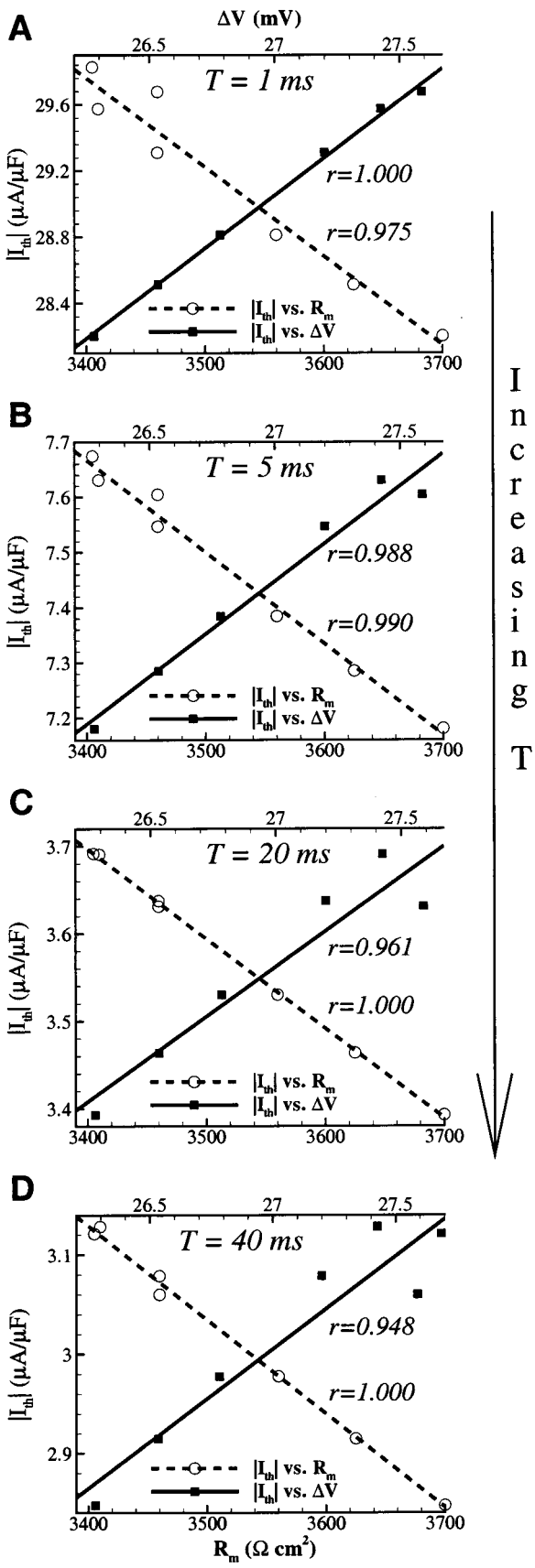

significant inactivation of I_{Na}, which elevates V_{th}, increases ΔV, and decreases excitability. This mechanism has been thoroughly discussed in the literature (Dominguez and Fozzard, 1970; Buchanan et al., 1985; Shaw and Rudy, 1997a) and will not be further investigated in this study. However, the role of R_m in excitability has not been as thoroughly explored as that of ΔV. Our results thus far suggest that changes in R_m are responsible for the dependence of excitability on pacing history for stimuli that are intermediate or long in duration ($T > 5$ ms). We next investigate the mechanism by which R_m itself depends on pacing history.

Mechanism of memory for a long duration stimulus: IV curves

We gain insight into how R_m and therefore excitability depend on pacing history for long T, by comparing current-voltage (IV) curves calculated after two different rates (Fig. 6 *A*) and two different durations (Fig. 6 *B*) of pacing. In Fig. 6 *A*, the IV curve after 100 beats of rapid pacing (S1S1 of 150 ms) is shifted downward relative to the IV curve after normal pacing (S1S1 of 300 ms). A downward shift of the curve results in an increase in R_m from 2670 Ωcm^2 to 2830 Ωcm^2 (the slope, $dI/dV = 1/R_m$, decreases) and a decrease in I_{th} from 2.63 $\mu A/\mu F$ to 2.37 $\mu A/\mu F$. In Fig. 6 *B*, the cell is paced rapidly for a longer period of time (2000 beats), and the IV curve shifts upward and to the right relative to the curve measured after 100 beats. Consequently, R_m decreases from 2830 Ωcm^2 to 2520 Ωcm^2 and I_{th} increases from 2.37 to 2.99 $\mu A/\mu F$.

The role of intracellular ionic concentrations in memory

We next examine intracellular ionic concentrations in cells with different pacing histories (Table 2) to understand the underlying ionic mechanism responsible for the shift of the IV curve and memory.

After 100 beats of rapid pacing, $[Ca^{2+}]_i$ accumulates to 0.29 μM compared to its value of 0.15 μM after 100 beats of normal pacing. This accumulation of intracellular Ca^{2+} increases the driving force for the Na^+-Ca^{2+} exchanger (I_{NaCa}) in the forward mode (to extrude Ca^{2+}). Due to the

FIGURE 4 Resting membrane resistance (R_m) and difference (ΔV) between $V_{m,rest}$ and V_{th} as determinants of excitability. Excitability is defined in terms of I_{th}, the minimum threshold current that elicits an excitatory response. The cell is paced for 100 times at seven different S1S1 intervals (2000, 1000, 300, 250, 200, 175, and 150 ms) after which R_m, I_{th}, and ΔV are all determined. I_{th} is plotted as a function of R_m (circles) and ΔV (squares) for four different values of stimulus duration, T: 1 ms (*A*), 5 ms (*B*), 20 ms (*C*), and 40 ms (*D*). Next to each linear fit of the data is shown the corresponding correlation coefficient, r. Note that for a short T, I_{th} and ΔV are highly correlated, whereas for a long T a greater correlation is achieved between I_{th} and R_m.

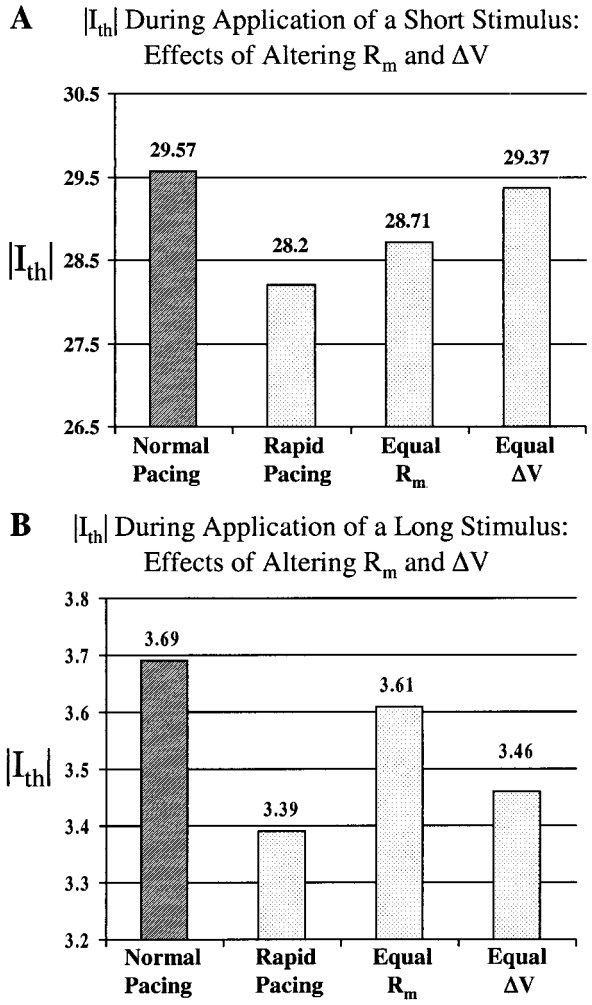

FIGURE 5 The effects of changing R_m and ΔV on excitability when I_{th} is measured with a short (*A*) and a long (*B*) duration stimulus. The cell is paced at a normal rate (S1S1 = 300 ms) for 100 beats after which I_{th} is determined by an S2 stimulus (*shaded column*). After rapid pacing (S1S1 = 150 ms), I_{th} is determined in the control situation (rapid pacing), with increased conductance of I_{K1} to eliminate rate-dependent differences in R_m (equal R_m), and with decreased conductance of I_{Na} to remove rate-dependent differences in ΔV (equal ΔV). Note that for a short T, eliminating changes in ΔV restores I_{th} to its control value. For a long T, a similar restoration of I_{th} occurs when changes in R_m are prevented.

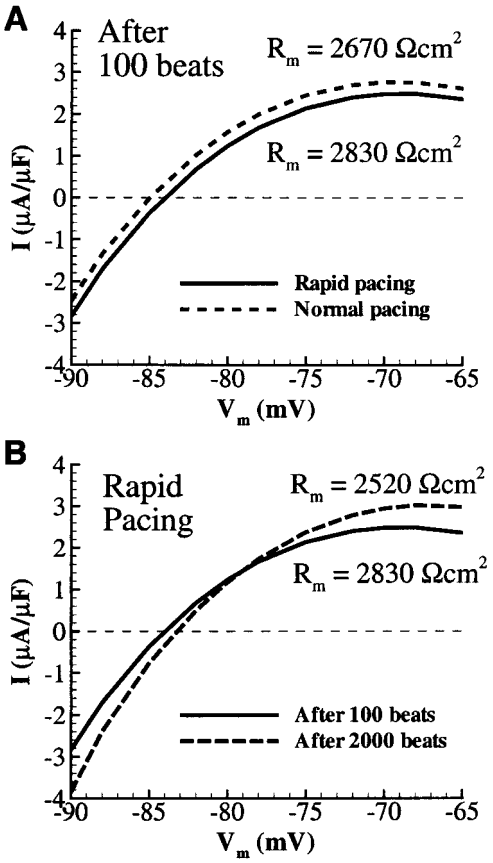

FIGURE 6 The dependence of the current-voltage curve on the rate and duration of pacing. Transmembrane current, I, is plotted as a function of membrane potential, V_m. Panel A compares the IV curve determined after pacing at an S1S1 of 150 ms (*solid line*) to that at an S1S1 of 300 ms (*dashed line*). Panel B shows IV curves for rapid pacing after 100 beats (*solid line*) and after 2000 beats (*long dashed line*). The corresponding R_m values are listed next to each curve.

stoichiometry of I_{NaCa} (Na^+:Ca^{2+} = 3:1), this results in an enhanced depolarizing current, which contributes to the downward shift of the IV curve after rapid pacing. Besides accumulation of $[Ca^{2+}]_i$, there is also depletion of $[Na^+]_i$ from 11.00 mM after normal pacing to 10.55 mM after rapid pacing (Table 2). The Na^+-K^+ pump, I_{NaK}, is an electrogenic ATPase that generates a net repolarizing current. Reduced intracellular Na^+ results in a smaller driving force for I_{NaK}, which reduces a repolarizing current and contributes to the downward shift of the IV curve after rapid pacing. Reduced Na^+ also increases I_{NaCa} in the forward mode (as does Ca^{2+} accumulation), adding to the downward shift of the IV curve. In summary, accumulation of Ca^{2+} and depletion of Na^+ after 100 beats of rapid pacing results in a downward shift of the IV curve. In Fig. 7 *A*, we test this hypothesis by resetting $[Na^+]i$ and $[Ca^{2+}]_i$ to their values after normal pacing. This manipulation shifts the IV curve upward and restores R_m and I_{th} to similar values calculated after normal pacing (2500 Ωcm^2 and 2.63 $\mu A/\mu F$, respectively, compared to 2520 Ωcm^2 and 2.63 $\mu A/\mu F$ in the control).

In Fig. 7, *B* and *C*, the cell is paced rapidly for a longer period of time (2000 beats). $[Ca^{2+}]_i$ accumulates from 0.29 μM after the 100th stimulus to 0.34 μM after the 2000th stimulus. However $[Na^+]_i$ increases from 10.55 to 14.12 mM, a 34% increase compared to only a 17% increase of $[Ca^{2+}]_i$. The result of a larger percentage increase in $[Na^+]_i$ relative to $[Ca^{2+}]_i$ is a reduced driving force for I_{NaCa} and a smaller depolarizing current. $[Na^+]_i$ accumulation also increases the activity of I_{NaK} which is a repolarizing current. These effects explain the upward shift of the IV curve after

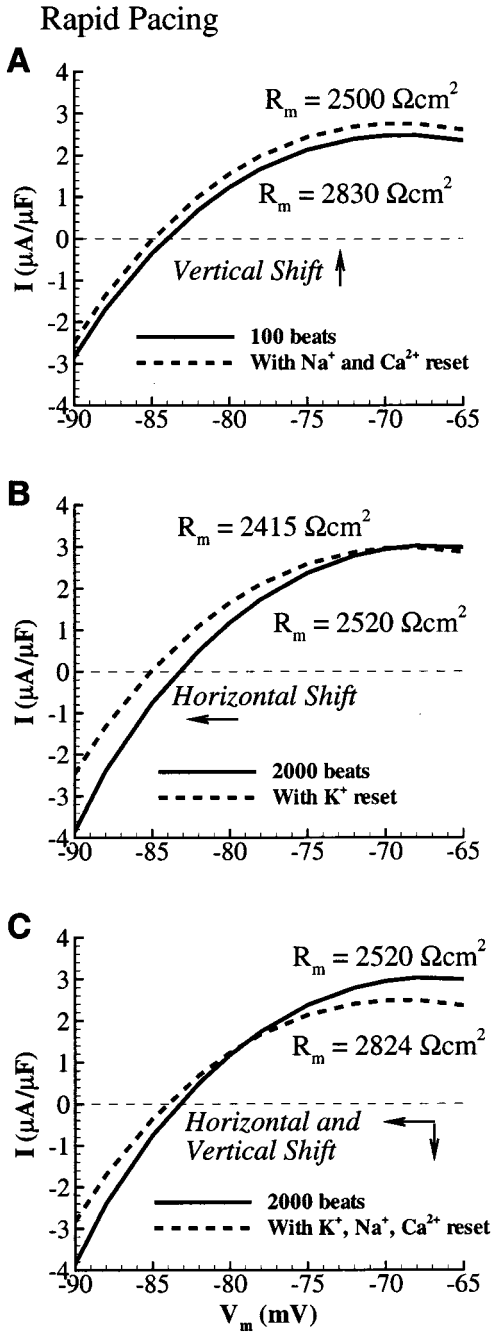

FIGURE 7 Effects of intracellular ion concentration changes on the IV curve. (*A*) IV curve after pacing the cell rapidly for 100 beats (solid line) is compared to the same IV curve measured but with $[Na^+]_i$ and $[Ca^{2+}]_i$ reset to their values after pacing at a normal rate (*dashed line*). (*B*) IV curve after rapid pacing for 2000 beats (*solid line*) is compared to the same IV curve but with $[K^+]_i$ reset to its value after 100 beats (*dashed line*). (*C*) Same as *B* except $[K^+]_i$, $[Ca^{2+}]_i$, and $[Na^+]_i$ are all reset to their values after 100 beats (*dashed line*).

a long duration of rapid pacing. In addition to changes in $[Ca^{2+}]_i$ and $[Na^+]_i$, there is depletion of $[K^+]_i$ from 142.89 to 132.51 mM, which elevates the I_{K1} reversal potential, E_{K1}, from −87.5 to −85.5 mV, shifting the IV curve to the right. Resetting $[K^+]_i$ to its value after 100 beats shifts the IV curve to the left (Fig. 7 *B*) and has very little effect on R_m or I_{th} (2415 Ωcm^2 and 2.88 μA/μF, respectively, compared to 2520 Ωcm^2 and 2.99 μA/μF in the control). However, additional resetting of $[Na^+]_i$ and $[Ca^{2+}]_i$ shifts the IV curve down (Fig. 7 *C*) and restores R_m and I_{th} to their values after 100 beats (2824 Ωcm^2 and 2.36 μA/μF, respectively, compared to 2830 Ωcm^2 and 2.37 μA/μF in the control).

DISCUSSION

Summary of findings

Important findings of this study are summarized here. i) As the stimulus duration, T, increases, excitability undergoes a transition from being ΔV-dependent to being R_m-dependent. ii) For long T, alterations in $\bar{g}_{K1}$, which modulate R_m, have a greater effect on excitability than do alterations in $\bar{g}_{Na}$. iii) The opposite is true for short T, where changes in $\bar{g}_{Na}$ modulate ΔV and more significantly affect excitability than do changes in $\bar{g}_{K1}$. iv) In the case of long T, changes in $[Na^+]_i$ and $[Ca^{2+}]_i$ affect R_m and excitability by shifting the IV curve in a vertical direction and are responsible for the dependence of excitability on the rate and duration of pacing (the memory effect).

R_m and ΔV as determinants of excitability

The major finding of this study that the determinants of excitability are dependent on T is consistent with experimental results and resolves an apparent conflict in the literature. As mentioned previously, Davidenko et al. (1990) propose that differences in R_m underlie changes in excitability. The strength-interval and current-voltage curves that they show to support their hypothesis are created with T = 20 ms. Our results show that R_m is indeed responsible for changes in excitability for long T (>5 ms). In contrast, studies during hyperkalemia support ΔV as the determinant of changes in excitability (Buchanan et al., 1985; Shaw and Rudy, 1997a). Slow conduction during hyperkalemia is due to reduced membrane excitability and does not involve long local delays (conduction delays across gap junctions are only about 1 ms; Shaw and Rudy, 1997a,c; Rohr et al., 1998). Therefore, the effective stimulus duration during such conduction is short. We conclude that ΔV is important in determining excitability for short T (5 ms or less). This observation supports the dominant role of ΔV in determining excitability during hyperkalemia. Indeed, the apparent conflict in the literature is resolved with the knowledge that there is a transition from ΔV-dependent to R_m-dependent excitability as T increases (Fig. 4).

Mechanism of memory: the IV curve

Schematic IV curves are presented in Fig. 8 to summarize how shifting of the IV curve affects R_m and I_{th}. The curve labeled 1 is the result of a horizontal shift of the control curve, drawn between curves 1 and 2 in Fig. 8. Notice that neither I_{th} nor the slope ($1/R_m$) of the curve near V_0 change in the case of a horizontal shift. Curve 2 is the result of a vertical shift of the control curve. A downward shift of the curve results in a decrease in I_{th} and an increase in R_m (the slope, $dI/dV = 1/R_m$, decreases). This analysis shows that a vertical shift of the IV curve results in altered R_m and excitability, whereas a horizontal shift changes V_0 without significantly affecting these parameters. According to Fig. 8, the vertical shift of the IV curve (due to $[Na^+]_i$ or $[Ca^{2+}]_i$ accumulation) is responsible for the dependence of R_m and excitability on the duration of pacing, whereas the rightward shift (due to $[K^+]_i$ depletion) has no effect. This agrees with results from our computer simulations (Fig. 7). Therefore, we conclude that $[Na^+]_i$ and $[Ca^{2+}]_i$ accumulation during pacing underlies the memory phenomenon associated with excitability changes.

Factors that affect R_m

Our results show that intracellular ionic concentration changes may affect cell excitability in the presence of a long stimulus by altering R_m. This may have serious implications during conditions of Ca^{2+} or Na^+ overload. For example, Ca^{2+} overload can lead to the initiation of delayed afterdepolarizations (Marban et al., 1986; Luo and Rudy, 1994b; Damiano and Rosen, 1984; Zeng and Rudy, 1995). As shown in this study, Ca^{2+} overload can also increase excitability by making I_{NaCa} more depolarizing and shifting the IV curve downward. This increase in excitability may further increase the likelihood of initiation and propagation of a delayed after-depolarization. Conversely, $[Na^+]_i$ accumulation tends to decrease R_m and excitability. The effects of either $[Na^+]_i$ or $[Ca^{2+}]_i$ accumulation on excitability may be blunted by the fact that they often occur in unison and have opposite effects on excitability.

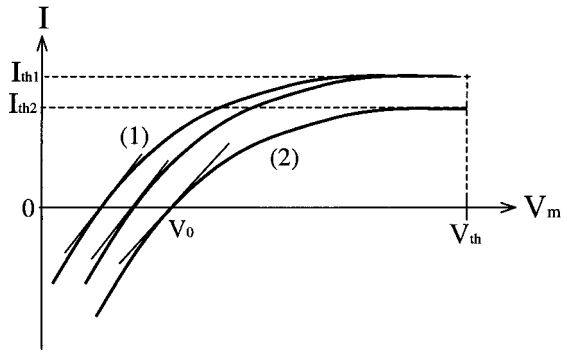

FIGURE 8 Schematic IV curves illustrating the effects of horizontal or vertical shifts of the curve on R_m and I_{th}. R_m is the reciprocal of the slope of the IV curve about V_0 and I_{th} is equal to $I(V_{th})$. Assuming that V_{th} is the same in all three cases, shifting the IV curve to the left (curve 1) of the control curve (shown between curve 1 and curve 2) has no effect on I_{th} or R_m. In contrast, shifting the IV curve downward (curve 2) decreases I_{th} and increases R_m.

Previous studies have hypothesized that during repetitive stimulation, the cellular response pattern (e.g., stimulus: response ratios and Wenckebach periodicity) is affected by a memory process that shortens action potential duration with time (Chialvo et al., 1990). Our simulations suggest that intracellular accumulation of Na^+ and Ca^{2+} underlies a slow memory process which may also affect the response of the cell to repetitive stimulation by shifting the SI curve in a vertical direction.

It is interesting to note that for long T, $[K^+]_i$ depletion has little effect on I_{th} even though it depolarizes $V_{m,rest}$ (Fig. 7 *B*). This is because $[K^+]_i$ affects E_{K1} but not $\bar{g}_{K1}$, resulting in a horizontal shift of the IV curve. As shown in Figs. 7 and 8, a horizontal shift of the IV curve does not affect excitability. Changes in $[K^+]_o$ were not investigated in this study, however $\bar{g}_{K1}$ shows a square root dependence on $[K^+]_o$. This suggests that hyperkalemia, as occurs during ischemia (Shaw and Rudy, 1997b), may affect excitability by altering R_m.

Memory processes in the heart

The memory effect discussed in this study is distinct from other forms of cardiac memory presented in the literature (for review, see Rosen et al., 1998) and from long term changes associated with electrical remodeling (for review, see Nattel, 1999). However, similarities exist between the underlying ionic processes of the memory phenomenon described here and other forms of short-term cardiac memory that involve modification of preexisting proteins by kinase activity (Rosen et al., 1998). Memory in this study also results from the response of channel proteins (Na^+-Ca^{2+} exchanger and Na^+-K^+ pump) to a time-dependent signal. However, the modulating signal here is a change in the concentrations of intracellular ions rather than an increase in kinase activity. We show that changes in intracellular ion concentrations are responsible for the memory effect in this study. The mechanism of cardiac memory (T-wave inversion during ventricular pacing) is still not fully determined (Rosen et al., 1998). It is possible that intracellular ion concentration changes, in addition to other stimuli, contribute to cardiac memory as well. It is also possible that the short-term memory described here, which develops over a few beats and involves ion transfer processes, may precede a cascade of other processes (e.g., phosphorylation) that lead to longer term effects underlying cardiac memory.

The memory effect described here is associated with a history of fast pacing over a period of time. In the heart,

cells can be subjected to repetitive rapid excitation during tachyarrhythmias. Since the result is altered cell excitability, the memory effect can modulate the excitatory responses of cardiac cells and tissue in a pro- or anti-arrhythmic fashion.

Relevance to pathophysiology

Our studies show that the transition from ΔV-dependent to R_m-dependent excitability occurs at about T = 5 ms. This suggests that during normal conduction or in cases of slow conduction that do not involve long local delays, ΔV is the primary determinant of excitability. Such situations arise during hyperkalemia, acute ischemia, or sodium channel blockade (Shaw and Rudy, 1997c). In contrast, the results suggest that during slow conduction involving long local delays (discontinuous propagation), R_m is the primary determinant of excitability, since the effective stimulus duration is long. Local conduction delays can occur as a result of structural changes due to tissue remodeling. Such changes can involve reduced gap-junction coupling, fibrosis, and the development of a highly heterogeneous substrate. Examples include aging (Spach and Dolber, 1986) and chronic ischemia and infarction (Ursell et al., 1985; Luke and Saffitz, 1991; Smith et al., 1991; Peters et al., 1998). The development of structural complexities and reduced gap-junction coupling can cause very long local conduction delays that are much longer than 5 ms (Shaw and Rudy, 1997c; Rohr et al., 1998; Kucera et al., 1998; Wang and Rudy, 2000). In addition, long local delays can develop at the tip of a spiral wave where the wavefront curvature is high (Fast and Kleber, 1997) or when the wavefront turns around a pivot point during reentry (Girouard et al., 1996).

The fact that excitability depends strongly on R_m in the arrhythmia-prone conditions listed above has implications for the development of effective anti-arrhythmic strategies. We have shown that under such conditions reducing $\bar{g}_{K1}$ increases excitability. Therefore, a drug that partially blocks I_{K1} could restore conduction in critical regions of conduction failure. It could also increase conduction velocity, thereby increasing the spatial extent of the action potential (the wavelength) and reducing the likelihood of initiation and sustenance of reentry.

We thank Dr. Niels Otani for many helpful discussions. This study was supported by grants R01-HL49054 and R37-HL33343 (to YR) from the National Heart, Lung and Blood Institute, National Institutes of Health, and by a Whitaker Foundation Development Award.

REFERENCES

Boyett, M. R., and B. R. Jewell. 1980. Analysis of the effects of changes in rate and rhythm upon electrical activity in the heart. *Prog. Biophys. Mol. Biol.* 36:1–52.

Buchanan, J. W., Jr., T. Saito, and L. S. Gettes. 1985. The effects of antiarrhythmic drugs, stimulation frequency, and potassium-induced resting membrane potential changes on conduction velocity and dV/dtmax in guinea pig myocardium. *Circ. Res.* 56:696–703.

Chialvo, D. R., D. C. Michaels, and J. Jalife. 1990. Supernormal excitability as a mechanism of chaotic dynamics of activation in cardiac Purkinje fibers. *Circ. Res.* 66:525–545.

Damiano, B. P., and M. R. Rosen. 1984. Effects of pacing on triggered activity induced by early afterdepolarizations. *Circulation.* 69: 1013–1025.

Davidenko, J. M., R. J. Levi, G. Maid, M. V. Elizari, and M. B. Rosenbaum. 1990. Rate dependence and supernormality in excitability of guinea pig papillary muscle. *Am J. Physiol.* 259:H290–H299.

Dominguez, G., and H. A. Fozzard. 1970. Influence of extracellular K+ concentration on cable properties and excitability of sheep cardiac Purkinje fibers. *Circ. Res.* 26:565–574.

Faber, G. M., and Y. Rudy. 2000. Action potential and contractility changes in [Na+]i overloaded cardiac myocytes: a simulation study. *Biophys. J.* 78:2392–2404.

Fast, V. G., and A. G. Kleber. 1997. Role of wavefront curvature in propagation of cardiac impulse. *Cardiovasc. Res.* 33:258–271.

Girouard, S. D., J. M. Pastore, K. R. Laurita, K. W. Gregory, and D. S. Rosenbaum. 1996. Optical mapping in a new guinea pig model of ventricular tachycardia reveals mechanisms for multiple wavelengths in a single reentrant circuit. *Circulation.* 93:603–613.

Jack, J. J. B., D. Noble, and R. W. Tsien. 1983. Electric Current Flow in Excitable Cells. Clarendon Press, Oxford.

Kucera, J. P., A. G. Kleber, and S. Rohr. 1998. Slow conduction in cardiac tissue. II. Effects of branching tissue geometry. *Circ. Res.* 83:795–805.

Luke, R. A., and J. E. Saffitz. 1991. Remodeling of ventricular conduction pathways in healed canine infarct border zones. *J. Clin. Invest.* 87: 1594–1602.

Luo, C. H., and Y. Rudy. 1991. A model of the ventricular cardiac action potential: depolarization, repolarization, and their interaction. *Circ. Res.* 68:1501–1526.

Luo, C. H., and Y. Rudy. 1994a. A dynamic model of the cardiac ventricular action potential. I. Simulations of ionic currents and concentration changes. *Circ. Res.* 74:1071–1096.

Luo, C. H., and Y. Rudy. 1994b. A dynamic model of the cardiac ventricular action potential. II. Afterdepolarizations, triggered activity, and potentiation. *Circ. Res.* 74:1097–1113.

Marban, E., S. W. Robinson, and W. G. Wier. 1986. Mechanisms of arrhythmogenic delayed and early afterdepolarizations in ferret ventricular muscle. *J. Clin. Invest.* 78:1185–1192.

Nattel, S. 1999. Atrial electrophysiological remodeling caused by rapid atrial activation: underlying mechanisms and clinical relevance to atrial fibrillation. *Cardiovasc. Res.* 42:298–308.

Noble, D., and R. B. Stein. 1966. The threshold conditions for initiation of action potentials by excitable cells. *J. Physiol. (Lond).* 187:129–162.

Peon, J., G. R. Ferrier, and G. K. Moe. 1978. The relationship of excitability to conduction velocity in canine Purkinje tissue. *Circ. Res.* 43:125–135.

Peters, N. S., J. Coromilas, M. S. Hanna, M. E. Josephson, C. Costeas, and A. L. Wit. 1998. Characteristics of the temporal and spatial excitable gap in anisotropic reentrant circuits causing sustained ventricular tachycardia. *Circ. Res.* 82:279–293.

Ravens, U., and H. M. Himmel. 1999. Drugs preventing Na+ and Ca2+ overload. *Pharmacol. Res.* 39:167–174.

Rohr, S., J. P. Kucera, and A. G. Kleber. 1998. Slow conduction in cardiac tissue, I: effects of a reduction of excitability versus a reduction of electrical coupling on microconduction. *Circ. Res.* 83:781–794.

Rosen, M. R., I. S. Cohen, P. Danilo, Jr., and S. F. Steinberg. 1998. The heart remembers. *Cardiovasc. Res.* 40:469–482.

Rosenbaum, M. B., H. H. Blanco, M. V. Elizari, J. O. Lazzari, and J. M. Davidenko. 1982. Electronic modulation of the T wave and cardiac memory. *Am. J. Cardiol.* 50:213–222.

Shaw, R. M., and Y. Rudy. 1997a. Electrophysiologic effects of acute myocardial ischemia: a mechanistic investigation of action potential conduction and conduction failure. *Circ. Res.* 80:124–138.

Shaw, R. M., and Y. Rudy. 1997b. Electrophysiologic effects of acute myocardial ischemia: a theoretical study of altered cell excitability and action potential duration. *Cardiovasc. Res.* 35:256–272.

Shaw, R. M., and Y. Rudy. 1997c. Ionic mechanisms of propagation in cardiac tissue: roles of the sodium and L-type calcium currents during reduced excitability and decreased gap junction coupling. *Circ. Res.* 81:727–741.

Smith, J. H., C. R. Green, N. S. Peters, S. Rothery, and N. J. Severs. 1991. Altered patterns of gap junction distribution in ischemic heart disease: an immunohistochemical study of human myocardium using laser scanning confocal microscopy. *Am. J. Pathol.* 139:801–821.

Spach, M. S., and P. C. Dolber. 1986. Relating extracellular potentials and their derivatives to anisotropic propagation at a microscopic level in human cardiac muscle. Evidence for electrical uncoupling of side-to-side fiber connections with increasing age. *Circ. Res.* 58:356–371.

Spear, J. F., and E. N. Moore. 1974. Supernormal excitability and conduction in the His-Purkinje system of the dog. *Circ. Res.* 35:782–792.

Ursell, P. C., P. I. Gardner, A. Albala, J. J. Fenoglio, Jr., and A. L. Wit. 1985. Structural and electrophysiological changes in the epicardial border zone of canine myocardial infarcts during infarct healing. *Circ. Res.* 56:436–451.

Viswanathan, P. C., R. M. Shaw, and Y. Rudy. 1999. Effects of IKr and IKs heterogeneity on action potential duration and its rate dependence: a simulation study. *Circulation.* 99:2466–2474.

Wang, Y., and Y. Rudy. 2000. Action potential propagation in inhomogeneous cardiac tissue: safety factor considerations and ionic mechanism. *Amer J. Physiol. (Heart).* 278:H1019–H1029.

Weidmann, S. 1952. The electrical constants of Purkinje fibers. *J. Physiol. (Lond).* 118:348–360.

Zeng, J., K. R. Laurita, D. S. Rosenbaum, and Y. Rudy. 1995. Two components of the delayed rectifier K+ current in ventricular myocytes of the guinea pig type. Theoretical formulation and their role in repolarization. *Circ. Res.* 77:140–152.

Zeng, J., and Y. Rudy. 1995. Early afterdepolarizations in cardiac myocytes: mechanism and rate dependence. *Biophys. J.* 68:949–964.